Journal of Materials Chemistry

Cite this: *J. Mater. Chem.*, 2012, **22**, 12358

www.rsc.org/materials

PAPER

Recoverable fluorescence chemosensors for Ni^{2+} ions based on hydrogen-bonded side-chain copolymers presenting pendent benzoic acid and pyridyl receptor units†

Po-Jen Yang, Hsuan-Chih Chu, Te-Cheng Chen and Hong-Cheu Lin*

Received 5th March 2012, Accepted 16th April 2012
DOI: 10.1039/c2jm31367g

In this study we synthesized the novel fluorescent conjugated homopolymers **P1** and **P4** and the copolymers **P2** and **P3** containing proton-acceptor (pyridyl receptor) **M1** monomer units and proton-donor (benzoic acid) **M2** monomer units and investigated them as recoverable chemosensors for Ni^{2+} ions (based on adjusting the fluorescence energy transfer between the **M1** and **M2** moieties through varying the degree of hydrogen bonding). The levels of available (*i.e.*, non-hydrogen-bonded) pyridyl receptors in the copolymers **P2** and **P3** were modified using different molar ratios of the pyridyl monomer **M1** and the benzoic acid monomer **M2**. Significant chelation of the Ni^{2+} ions by the fluorescent homopolymers **P1** and **P4** and the copolymers **P2** and **P3** was evident by their distinct fluorescence quenching behaviors; the specific quenching constants (K_{SV}) decreased in the order **P1** > **P2** > **P3** > **P4**, following the trend of the molar ratios of pyridyl receptors. When we added a third component, cyclodextrin (CD), to cap the benzoic acid moieties and, thereby, disrupt the hydrogen bonding between the **M1** and **M2** moieties in the copolymers **P2** and **P3**, the levels of available pyridyl receptors in the recoverable chemosensor copolymers increased, resulting in relatively higher quenching constants for the **P2** + CD, **P3** + CD and blend (**P1**/**P4**) + CD systems. Fluorescence decay experiments revealed that the addition of CD also increased the fluorescence quenching efficiencies of the copolymers **P2** and **P3** towards Ni^{2+} ions. Such supramolecular (hydrogen-bonded) side-chain fluorescent copolymers might have practical applicability as recoverable and/or adjustable chemosensors.

Introduction

Many chemo- and bio-sensor materials have been developed recently to measure values of pH and detect metal ions and biological species based on changes in their fluorescence signals.[1,2] Among them, chemosensors derived from conjugated polymers have attracted considerable attention because their fluorescence properties respond significantly to coupling between the polymer's receptors and the detected analytes. Polymeric chemosensors typically exhibit an amplifying mechanism as a result of energy transfer of excitons among the conjugated chains; as a result, most conjugated polymeric sensors are more sensitive than their small-molecule counterparts.[3] Moreover, the responses of multi-receptor polymeric systems featuring collective interactions are generally stronger than those of mono-receptor small-molecule systems featuring single interactions. Several fluorescent polymeric sensors have been developed to interact selectively with particular ions.[4–6] Some polymeric fluorescence sensors were reported to explain their photo-physical phenomena, such as electron and/or energy transfer processes.[7] Furthermore, receptors featuring various functional segments can be included in copolymeric sensors to extend their applicability.[8] The molecular design of copolymers offers the ability not only to vary the fluorescence intensities and/or wavelengths of the individual fluorophores to different degrees but also to add additional logic signals (or functions) through the incorporation of other responsive segments in the copolymer chains.[9] Special photophysical properties can be produced by the twisted intramolecular charge transfer (TICT) phenomena of 4-(*N*,*N*-dimethylamino)benzonitrile (DMABN)[10] and its derivatives[11] in the hydrophobic cavities of cyclodextrin (CD). In particular, the dependence of the TICT emissions on the environmental polarity, viscosity and rotational mobility of the donor moieties makes these molecules (*e.g.*, DMABN) excellent candidates[12] for examining microscopic molecular environments. The excited state dynamics of DMABN units positioned within the cavities of CDs[13] vary with respect to those in solution because of the low polarity of the cavity and the geometric constraints. The reduced polarity and restricted environment of the CD medium can be used to tune the position and intensity of the distinct band of a fluorophore, due to the

Department of Materials Science and Engineering, National Chiao Tung University, Hsinchu, Taiwan (ROC). E-mail: linhc@cc.nctu.edu.tw; Fax: +8863-5724727; Tel: +8863-5712121 ext. 55305

† Electronic supplementary information (ESI) available: Synthesis and characterization of monomer **M2**. See DOI: 10.1039/c2jm31367g

energy difference between the locally excited state and internal charge transfer (ICT) state. For example, the photophysical properties of *p*-dimethylaminobenzoic acid,[14] *p*-aminobenzoic acid,[15] *o*-aminobenzoic acid[16] and *m*-aminobenzoic acid[17] have been investigated in CD systems.

In this study, we employed two conjugated monomeric fluorophores—one featuring a pyridyl receptor and the other a benzoic acid moiety—to prepare corresponding homopolymers and copolymers as recoverable (and/or adjustable) chemosensors for the detection of metal ions (see Fig. 1). Based on our previous report,[18] we prepared the proton-acceptor monomer **M1** bearing a conjugated pyridyl receptor for coordination with metal ions. As illustrated in Scheme 1, we synthesized the proton-donor monomer **M2** bearing a conjugated benzoic acid unit for binding in the cavities of β-CD moieties, and its detailed synthetic procedures and characterization are demonstrated in the ESI†. Scheme 2 outlines the preparation of the copolymers **P2** and **P3** with different molar ratios of **M1** and **M2** units ($x : y = 1 : 0.1$ and $1 : 0.8$, respectively) and the homopolymers **P1** and **P4** (from monomers **M1** and **M2**, respectively). The degrees of supramolecular (hydrogen-bonding) interactions between the **M1** and **M2** units were tuned by varying their molar ratios or by adding CDs. Because the benzoic acid moieties in the **M2** units of the copolymers **P2** and **P3** would bind to the CDs, we could use the addition of CDs to control the degrees of supramolecular interactions (between monomers **M1** and **M2**) as well as the metal ion coordination by the free (non-hydrogen-bonded) pyridyl moieties of the **M1** units in the copolymers **P2** and **P3**. Because the coordination of pyridyl receptors with different metal ions affects their fluorescence properties, we could construct a model to determine the sensing contributions of the pyridyl receptors of the **M1** units in the homopolymer **P1** towards metal ions and found the best sensing selectivity of Ni^{2+} ions in our previous study.[18] The intriguing photophysics of the polymeric fluorophores upon complex formation in constrained CDs provoked us to explore the photoluminescence (PL) emissions of the benzoic acid moieties of the **M2** units in the copolymers **P2** and **P3** and the homopolymer **P4**. Based on characteristic changes in PL emissions, we monitored the Ni^{2+} ion sensitivities of the copolymers **P2** and **P3** in the presence and absence of CDs. Moreover, as model chemosensors for specific metal Ni^{2+} ions or biomolecules, we employed benzoic acid moieties in these

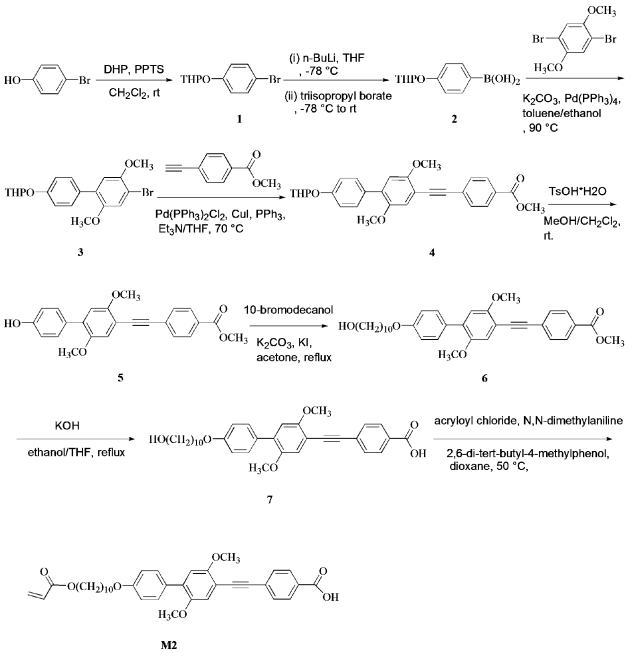

Scheme 1 Synthetic route towards monomer **M2**.

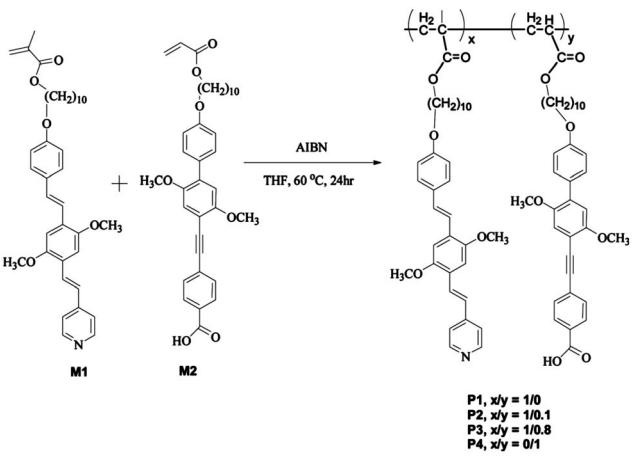

Scheme 2 Synthetic route towards polymers **P1–P4**.

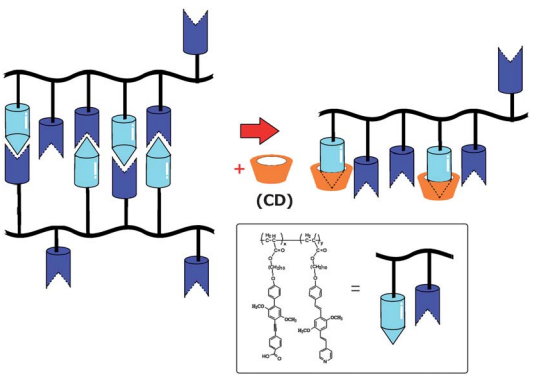

Fig. 1 Schematic representation of the release of pyridyl receptors, for the sensing of metal ions in recoverable chemosensor copolymers bearing pendent benzoic acid and pyridyl receptor units, upon adding CDs to cap the benzoic acid moieties.

copolymers to ensure the feasibility of energy transfer between these proton donors and the pyridyl proton acceptors. In suitable proton donor–acceptor combinations, we envisioned the tunable sensing capabilities of chemosensors towards particular analytes (*e.g.*, metal ions and biomolecules). In addition, more-efficient energy transfer, resulting in larger PL emission contrasts or broader sensing concentration ranges, should ensue in the coordinated (analyte-attached) states of polymeric chemosensors during the sensing process.

Experimental

Materials

Chemicals and solvents of reagent grade were purchased from Aldrich, ACROS, TCI, and Lancaster Chemical. Tetrahydrofuran

(THF) and triethylamine (Et_3N) were dried and distilled prior to use. Azobisisobutyronitrile (AIBN) was recrystallized from MeOH prior to use. The other chemicals were employed without further purification. The monomer **M1** was prepared according to the literature.[18]

Measurements and characterization

^{1}H NMR spectra were recorded using a Varian Unity 300 MHz spectrometer with $CDCl_3$ and DMSO-d_6 as solvents. Elemental analyses were performed using a HERAEUS CHN-OS RAPID elemental analyzer. High-resolution electron impact mass spectra were recorded using a Finnigan-MAT-95XL apparatus. Gel permeation chromatography (GPC) was performed using a Waters HPLC pump 510 connected to a Waters 410 differential refractometer and three Ultrastyragel columns, with polystyrene as a standard and THF as an eluent. UV-Vis absorption spectra were recorded using an HP G1103A spectrophotometer; PL spectra of dilute THF solutions (5×10^{-6} M) were recorded using a Hitachi F-4500 spectrophotometer. Time-resolved photoluminescence (TRPL) spectra were measured using a home-built single photon counting system with excitation from a 375 nm diode laser (Picoquant PDL-200, 50 ps fwhm, 2 MHz). The signals collected at the excitonic emissions of polymer solutions ($\lambda = 480$ nm) were connected to a time-correlated single photon counting card (TCSPC, Picoquant Timeharp 200). The emission decay data were analyzed with biexponential kinetics, from which two decay components were derived; the lifetimes (τ_1, τ_2) and pre-exponential factors (A_1, A_2) were determined.

General procedure for the synthesis of the copolymers P2 and P3 and the homopolymer P4

A mixture (1.5 g) of the monomers **M1** and **M2** was dissolved in dry THF (7.5 mL) in a Schlenk tube, with a monomer concentration of 20 wt%, and then AIBN (2 mol% of total monomer concentration) was added as an initiator. The solution was degassed through three freeze/pump/thaw cycles and then the tube was sealed off. The mixture was stirred at 60 °C for 24 h and then precipitated into Et_2O. The precipitated polymer was collected, washed with Et_2O and dried under high vacuum.

P2 (**M1**–**M2**$_{0.8}$). ^{1}H NMR (300 MHz, DMSO-d_6): δ (ppm) 8.47 (br, 2H), 7.96–6.76 (br, 16H), 3.88 (br, 18H), 1.78–1.51 (br, 32H).

P3 (**M1**–**M2**$_{0.1}$). ^{1}H NMR (300 MHz, DMSO-d_6): δ (ppm) 8.46 (br, 2H), 7.93–6.75 (br, 11H), 4.33–3.83 (br, 11H), 1.73–1.52 (br, 23H).

P4 (**M2**). ^{1}H NMR (300 MHz, DMSO-d_6): δ (ppm) 8.08 (br, 2H), 7.67–6.87 (br, 8H), 4.15–3.74 (br, 10H), 1.80–1.54 (br, 14H).

Metal Ni^{2+} ion and CD titrations

The metal Ni^{2+} ion and CD titrations were performed using polymer solutions (5.0×10^{-6} M) in THF (150 mL) and solutions of Ni^{2+} ions (1×10^{-3} M of $NiCl_2$ in THF containing 3 vol% H_2O) and β-CD (3×10^{-3} M in THF containing 25 vol% EtOH and 25 vol% H_2O). The fluorescence titration spectra were recorded after titration for 7 min to allow complete formation of complexes between the Ni^{2+} ions and the polymers.

Metal ion-induced fluorescence quenching of polymers

The PL quenching behavior followed the Stern–Volmer (SV) equation

$$I_0/I = 1 + K_{SV}[Q]$$

where I_0 and I are the emission intensities of the fluorescent polymer in the absence and presence, respectively, of the quencher Q (Ni^{2+} ions), K_{SV} is the SV quenching constant, and [Q] is the concentration of the quencher.

Results and discussion

Synthesis and characterization of polymers

The proton-acceptor monomer **M1** containing three conjugated aromatic rings, including one pyridyl terminus for coordination with metal ions, was prepared using Wittig and Pd-catalyzed Heck couplings.[18,19] The proton-donor monomer **M2** bearing three conjugated aromatic rings, including one terminal benzoic acid moiety for interacting with CDs to tune the fluorescence, was synthesized as indicated in Scheme 1. The homopolymers **P1** and **P4** and the copolymers **P2** and **P3** were prepared (Scheme 2) through radical polymerizations of mixtures of the proton-acceptor (pyridyl) monomer **M1** and the proton-donor (benzoic acid) monomer **M2**.[20] Most importantly, the fluorescence of the copolymers **P2** and **P3** could be recovered and/or adjusted through coordination of the benzoic acid units of the **M2** moieties with CDs, thereby allowing control over the chemosensor's sensitivities towards metal ions (through variations in fluorescence energy transfer between the **M1** and **M2** moieties at different degrees of hydrogen bonding). In a previous study, we established the presence of hydrogen bonding between carboxylic acid and pyridine units in polymers.[21] In the present study, we used the homopolymer **P1** as a model compound because we had demonstrated previously its effective fluorescence chemosensor capability, allowing it to distinguish the presence of metal Ni^{2+} ions (with the maximum selectivity) through interactions with its pendent pyridyl receptors.[18] The detailed synthesis of the proton-donor (benzoic acid) monomer **M2** is outlined in the ESI†. Compound **1** was prepared from 4-bromophenol and 3,4-dihydro-2*H*-pyran (DHP); subsequent bromine–lithium exchange (using *n*-BuLi) and boronation (with 2-isopropoxy-4,4,5,5-teramethyl-1,3,2-dioxaborolane) gave **2**. Suzuki coupling between **2** and 1,4-dibromo-2,5-dimethoxybenzene yielded **3**. Compound **4** was synthesized from **3** through Sonogashira coupling with 4-ethynylbenzoic acid methyl ester; deprotection of the THPO protecting group (with *p*-TsOH) provided **5**, which we reacted with 10-bromodecanol to give **6**; hydrolysis of the ester yielded the carboxylic acid **7**. Finally, **M2** was obtained through the acylation of **7** with acryloyl chloride. The polymerization of **M1** and **M2** was performed through conventional free radical polymerization in THF at 60 °C, using AIBN as the initiator. The product molar ratios of the monomer units **M1** to **M2** in **P1**–**P4** were verified, using NMR spectroscopy, to be 1 : 0, 1 : 0.1, 1 : 0.8, and 0 : 1, respectively. In the ^{1}H NMR spectra of the polymers, the disappearance of the signals for the vinyl (*i.e.*, acrylate) protons at 5.5–6.0 ppm indicated the complete consumption of the monomers. We estimated the

copolymer compositions of **P1–P4** by comparing the relative integration of the signals at 8.4 ppm (corresponding to two protons of the pyridyl groups of the **M1** units) and 6.8–7.9 ppm (corresponding to the other overlapped aromatic protons of the **M1** and **M2** units). The product compositions of copolymers **P2** and **P3** were very close to the feeding ratios of the monomers. All of the polymers were soluble in common organic solvents, including THF, DMSO, and DMF. The weight-average molecular weights (M_w) and polydispersity indexes (PDIs) of the polymers **P1–P4**, determined through GPC, were in the ranges 9.7–37.4 kg mol^{-1} and 1.18–2.11, respectively. Table 1 summarizes the compositions (input and output molar ratios), molecular weights (M_w), PDIs, and yields of **P1–P4**.

Photophysics of polymers P1–P4

As reported previously, the fluorescent conjugated homopolymer **P1** containing the proton-acceptor (pyridyl) monomer **M1** is an ideal reversible chemosensory material.[18] In this study, we prepared the homopolymer **P4** and the copolymers **P2** and **P3** to investigate their abilities to function as recoverable chemosensors for metal ions (through tunable fluorescence energy transfer between the **M1** and **M2** moieties upon varying the degrees of hydrogen bonding); Table 2 summarizes the photophysical properties of these polymers. The PL quantum yields (Φ_{PL}) of the polymers **P1–P4** in dilute THF solutions were in the range 0.41–0.57, depending on the content of **M2** moieties. The fluorescence of the copolymers **P2** and **P3** could be tuned by disrupting the hydrogen bonding between the **M1** and **M2** moieties through the stronger interactions of the **M2** (benzoic acid) moieties with CDs, thereby controlling the sensitivities of these chemosensors towards metal ions; therefore, we investigated the adjustable fluorescence energy transfer between the **M1** and **M2** moieties at various degrees of hydrogen bonding in the copolymers **P2** and **P3**.

In Fig. 2, we assigned the absorption bands of the polymer **P1** near 332 and 400 nm to the **M1** (pyridyl receptor) units. In addition, the absorption intensities of the polymers **P2–P4** (in THF) near 320 nm (attributed to **M2**) increased gradually relative to those near 400 nm (attributed to **M1**), proportionally to the content of **M2** (benzoic acid) units. Fig. 3 presents the PL emission spectra of the polymers **P1–P4** in THF; Table 2 lists the pertinent data. The homopolymers **P1** and **P4** (containing **M1** and **M2** moieties, respectively) exhibited their maximum PL emissions near 467 and 401 nm, respectively. The PL emission intensities of the copolymers **P2** and **P3** (in THF) near 463 and 403 nm are related to their **M1** and **M2** contents, respectively. The PL emission peaks near 403 nm (from **M2** moieties) were weaker than those near 463 nm (from **M1** moieties) for the copolymers **P2** and **P3**, which implied efficient energy transfer occurred from the **M2** moieties to the **M1** moieties. In order to probe this energy transfer effect, the photoluminescent

Table 2 Absorption and PL emission spectral data of polymers **P1–P4** in THF solutions

Polymer	$\lambda_{abs,sol}$[a] (nm)	$\lambda_{PL,sol}$[ab] (nm)	Φ_{PL}[c]
P1	332, 400	467	0.41
P2	333, 399	401, 463	0.43
P3	327, 402	404, 462	0.49
P4	320	403	0.57

[a] Measured in dilute THF solutions. [b] Excited at the maximum absorption wavelength of each polymer. [c] Solution PL quantum yields (Φ_{PL}) were measured in THF, relative to 9,10-diphenylanthracene ($\Phi_{PL} = 0.90$).

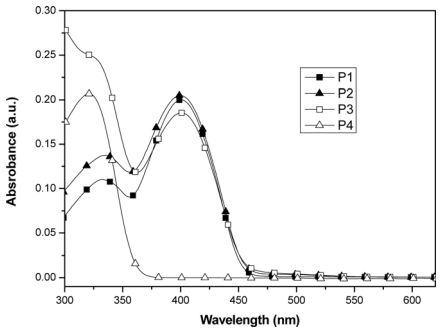

Fig. 2 Absorption spectra of the polymers **P1–P4** (5×10^{-6} M in THF).

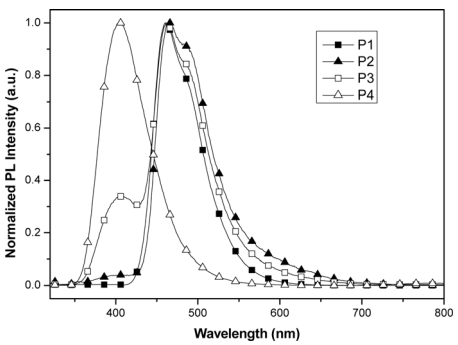

Fig. 3 Normalized PL spectra of the polymers **P1–P4** (5×10^{-6} M in THF).

Table 1 Compositions, yields, molecular weights, and degradation temperatures of polymers **P1–P4**

	Molar ratio				
Polymer	Feeding (**M1**/**M2**)	Product (x/y)[a]	Yield (%)	M_w (g mol^{-1})[b]	PDI (M_w/M_n)[b]
P1	1/0	1/0	65	11 200	1.70
P2	1/0.1	1/0.1	64	9707	2.11
P3	1/1	1/0.8	69	11 950	1.42
P4	0/1	0/1	40	37 441	1.18

[a] Determined from ^{1}H NMR spectra. [b] Weight-average molecular weight (M_w) and polydispersity index (PDI) determined by GPC in THF using polystyrene standards.

excitation (PLE) and absorption spectra of the copolymer **P3** in THF solutions were recorded in Fig. S1 (ESI†). In contrast to **P3**, the absorption and PL emission spectra of homopolymer **P4** in THF solutions are illustrated as well. The absorption spectrum of copolymer **P3** overlapped significantly with the PL emission spectrum of **P4**, suggesting that energy transfer from the **M2** moieties to the **M1** moieties should be expected. The feature in the PLE spectrum of **P3** appears to match that in the corresponding absorption spectra of **P3**, where the PLE spectrum was monitored at the corresponding maximum PL emission. These measurements conclusively revealed the energy transfer from the benzoic acid (**M2**) moieties to the pyridyl receptors (**M1**) in the copolymer **P3**. Furthermore, we might expect supramolecular interactions between the **M1** and **M2** moieties (*via* hydrogen bonds) to further facilitate energy transfer in the copolymers **P2** and **P3** (in THF), providing a window to study the recoverable and/or adjustable sensitivities of the chemosensors and photoinduced energy transfer between proton donor and acceptor moieties.

Fluorescence quenching of polymers upon titration with Ni^{2+} ions

As in our previous report,[18] among the variety of tested metal ions (including Cu^{2+}, Fe^{3+}, Fe^{2+}, Ni^{2+}, Au^{3+}, Mn^{2+}, Mg^{2+}, Cr^{2+}, and Hg^{2+}), the homopolymer **P1** (containing only pyridyl receptors for metal ions) exhibited its best chemosensing capability towards Ni^{2+} ions, as measured through fluorescence quenching titration experiments; the fluorescence intensity of **P1** decreased dramatically upon the addition of Ni^{2+} metal ions as a result of complexation of the fluorescent pyridyl units with the Ni^{2+} ions. Therefore, in this study we chose[18] to investigate the chemosensor capabilities of the homopolymers **P1** and **P4** and the copolymers **P2** and **P3**. In the fluorescence quenching experiments in Fig. 4, the PL spectra of the homopolymers **P1** and **P4** and the copolymers **P2** and **P3** (each 5×10^{-6} M in THF) were monitored in the presence of Ni^{2+} ions with the same concentration (1.1×10^{-6} M). The fluorescence spectra of the homopolymers **P1** and **P4** exhibited maximum PL emissions at 464 and 403 nm, respectively. In Fig. 4(a) and (b), the copolymers **P2** and **P3** with benzoic acid moieties titrated with Ni^{2+} ions exhibited PL quenching trends similar to those of the homopolymer **P1** suggesting that the complexation of the pyridyl units in the copolymers **P2** and **P3** with the Ni^{2+} ions was similar to the interactions of **P1**. Because of hydrogen bonding of the proton-accepting pyridyl receptors of the **M1** units with the proton-donating benzoic acid moieties of the **M2** units in the copolymers **P2** and **P3**, the content of available pyridyl receptors (*i.e.*, not hydrogen bonded to benzoic acid moieties and, therefore, free to complex with Ni^{2+} ions) in **P2** and **P3** would be much lower than that in the homopolymer **P1**. Consequently, the PL quenching effect of the Ni^{2+} ions on the copolymers **P2** and **P3** was much weaker than that on the homopolymer **P1**. In a previous study, we reported a similar PL quenching phenomenon for gold nanocomposites interacting with fluorescent homopolymers and copolymers; in that case, hydrogen bonding of the monomer moieties in the copolymer resulted in a lower quenching efficiency of the gold nanoparticles towards the copolymer.[21]

Because of the greater availability of the pyridyl receptors (*i.e.*, non-hydrogen-bonded and, therefore, free to complex with metal ions) in **P2**, which featured a lower ratio of benzoic acid moieties (*i.e.*, monomer **M2** units), the quenching effect of **P2** was greater than that of **P3** when titrated with Ni^{2+} ions. We prepared a polymer blend (**P1**/**P4**) from the homopolymers **P1** and **P4** such that it featured a molar ratio of its monomer unit similar to that of the copolymer **P2** ($x : y = 1 : 0.1$). Fig. 4(c) reveals that the quenching effect of **P2** was greater than that of the blend (**P1**/**P4**) when titrated with Ni^{2+} ions, indicating that the hydrogen bonding interactions among the homopolymers **P1** and **P4** of the blend (**P1**/**P4**) were stronger than those in the copolymer **P2**. In contrast to the situation for the homopolymer **P1**, no complexation occurred between **P4** and Ni^{2+} ions [Fig. 4(d)], due to the lack of pyridyl receptors in the homopolymer **P4** (featuring only benzoic acid moieties); therefore, no obvious fluorescence quenching occurred upon the addition of Ni^{2+} ions. Hence, according to the fluorescence quenching results, the excitons of the homopolymer **P1** were more readily trapped through charge-transfer to the Ni^{2+} ions than were those of the copolymers **P2** and **P3**. Fig. 5(a)–(d) present Stern–Volmer (SV) plots—replotted from Fig. 4(a)–(d), respectively—of the copolymers **P2** and **P3**, the blend (**P1**/**P4**), and the homopolymers **P4** titrated with the same concentration (up to 1.1×10^{-6} M in THF) of Ni^{2+} ions; Table 3 lists the corresponding quenching constants (K_{SV}) acquired from these SV plots. From the SV plots, the detection limits of polymers without CDs for Ni^{2+} ions were in the range of 0.11–0.16 $\times$ 10^{-6} M. According to Fig. 5(a) and (b), the quenching constants for the copolymers **P2** and **P3** (1.67×10^6 and 4.91×10^5 M^{-1}, respectively) titrated with Ni^{2+} ions were lower than that of the homopolymer **P1** (5.65×10^6 M^{-1}), due to the lower availability of metal Ni^{2+} ion receptors (*i.e.*, non-hydrogen-bonded pyridine units) in the copolymers **P2** and **P3** for complexation with Ni^{2+} ions. Based on Fig. 5(c), the quenching constant (3.72×10^5 M^{-1}) of the blend (**P1**/**P4**) was lower than that (1.67×10^6 M^{-1}) of the copolymer **P2** [at a similar molar ratio of monomer units ($x : y = 1 : 0.1$)] when titrated with Ni^{2+} ions, confirming that the lower availability of the free pyridyl receptors occurred in the blend (**P1**/**P4**) because of its stronger hydrogen bonding interactions. Moreover, the lack of pyridyl receptors in the homopolymer **P4**, featuring only proton-donating benzoic acid units, provided a quenching constant of 3.62×10^4 M^{-1}, calculated from the SV plot in Fig. 5(d), that was much lower than that of the homopolymer **P1**. Hence, both (i) complexation of the pyridyl receptors with the metal ions and (ii) hydrogen bonding between the proton-acceptor pyridyl receptors (of monomer **M1** units) and proton-donor benzoic acid moieties (of monomer **M2** units) played important roles in the fluorescence quenching of the copolymers **P2** and **P3**. In general, we could distinguish the significant chelation between the metal ions and the fluorescent homopolymers **P1** and **P4** as well as the copolymers **P2** and **P3** in terms of distinct fluorescence quenching behaviors with specific quenching constants (K_{SV}).

Fluorescence quenching of polymers in the presence of CDs upon titration with Ni^{2+} ions

In contrast to the behavior of the fluorescent homopolymer **P1**, which does not undergo self-complexation through hydrogen bonding, the introduction of proton-donor benzoic acid moieties (of monomer **M2** units) to the copolymers **P2** and **P3** resulted in

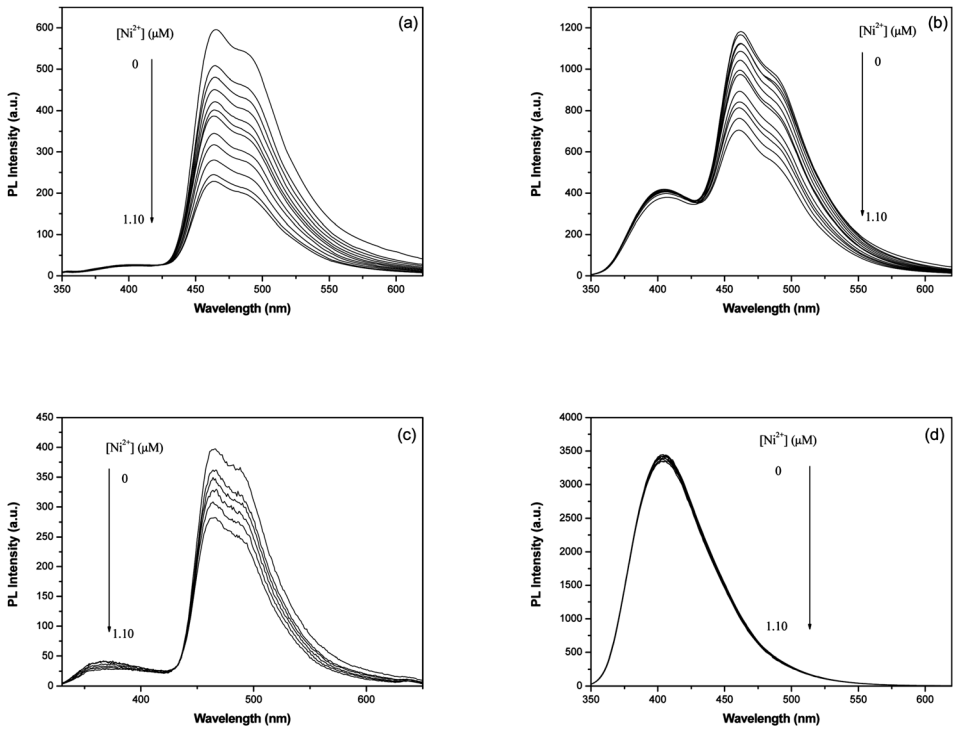

Fig. 4 Fluorescence quenching spectra of polymers **P1**–**P4** titrated with the same concentration (up to 1.1×10^{-6} M in THF) of Ni^{2+} ions: (a) **P2**, (b) **P3**, (c) blend (**P1**/**P4**), and (d) **P4** in THF solutions (5×10^{-6} M).

hydrogen-bonded interactions between the proton-accepting pyridyl receptors (of monomer **M1** units) and proton-donating benzoic acid moieties (of monomer **M2** units). As a result, the content of available (*i.e.*, non-hydrogen-bonded) pyridyl receptors could be adjusted by varying the copolymer design to feature different molar ratios of the proton-acceptor and proton-donor units, as we have

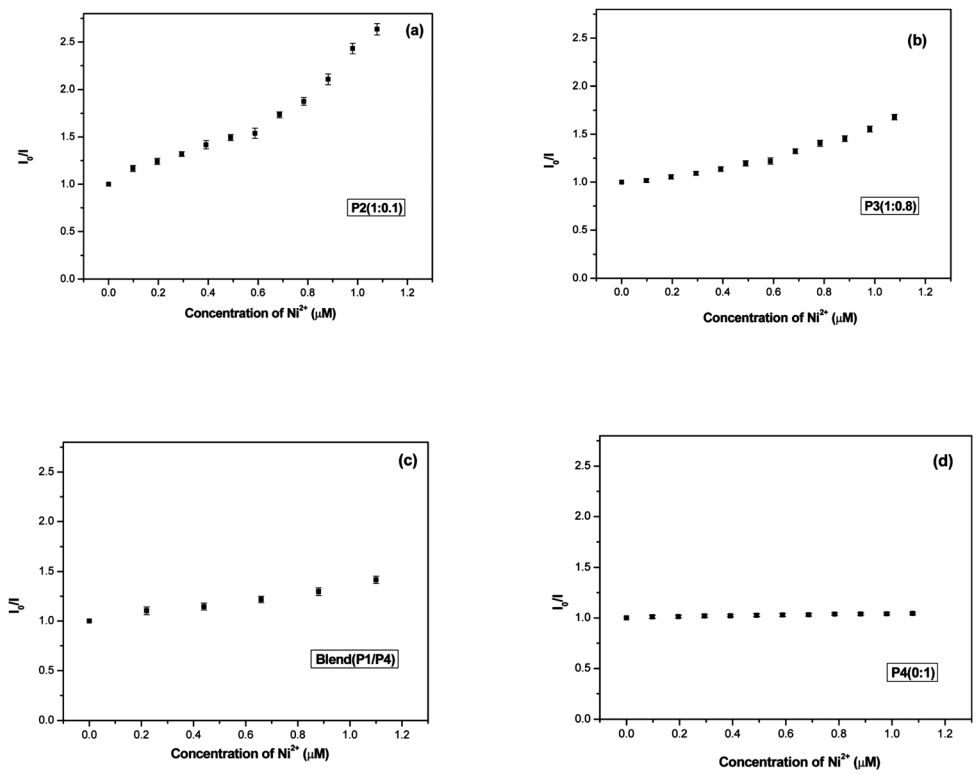

Fig. 5 SV plots of polymers, in THF solutions (5×10^{-6} M), titrated with the same concentration (up to 1.1×10^{-6} M in THF) of Ni^{2+} ions: (a) **P2**, (b) **P3**, (c) blend (**P1**/**P4**), and (d) **P4**.

Table 3 Values of K_{SV} for polymers titrated with Ni^{2+} ions

Polymer	Components (x : y)	K_{SV} (M^{-1})[a]
P1[b]	1 : 0	5.65×10^6
P2	1 : 0.1	1.67×10^6
P3	1 : 0.8	4.91×10^5
P4	0 : 1	3.62×10^4
Blend (**P1/P4**)	1 : 0.1	3.72×10^5
P1 + CD	1 : 0	5.11×10^6
P2 + CD	1 : 0.1	4.76×10^6
P3 + CD	1 : 0.8	2.81×10^6
Blend (**P1/P4**) + CD	1 : 0.1	5.02×10^5

[a] The PL quenching efficiency can be evaluated through the static SV quenching constant (K_{SV}), monitoring the corresponding decreases in PL intensity upon increasing the metal ion concentration in the linear region, according to the well-known static SV equation: $I_0/I = 1 + K_{SV}[Q]$, where I_0 is the PL intensity in the absence of the quencher, I is the PL intensity in the presence of the quencher, and [Q] is the quencher concentration. [b] The value of K_{SV} for **P1** was obtained from our previous report.[18]

demonstrated herein with the copolymers **P2** and **P3**. An alternative approach is to add a third component, namely a CD, to cap the benzoic acid moieties and, thereby, weaken the hydrogen bonding between the **M1** and **M2** moieties to different extents in the copolymers **P2** and **P3**. Accordingly, the levels of free pyridyl receptors could be increased through capture of the benzoic acid moieties (of monomer **M2** units) by the CDs, allowing the development of the first recoverable chemosensor copolymers **P2** and **P3**. To prove the capabilities of the recoverable chemosensors, we studied the fluorescence quenching properties of the copolymers **P2** and **P3** and the blend (**P1/P4**) titrated with Ni^{2+} ions in the presence of CDs. Fig. 1 displays the mechanism behind the release of the pyridyl receptors in the hydrogen-bonded copolymers **P2** and **P3** after the addition of CDs.

Upon the addition of CDs at certain concentrations, the benzoic acid moieties (of monomer **M2** units) were captured by the CDs, such that some of the quenched hydrogen-bonded pyridyl receptors were released; thus, both (i) the non-hydrogen-bonded pyridyl receptors and (ii) the benzoic acid units capped by CDs exhibited enhanced fluorescence to different degrees. As illustrated in Fig. 6(a), the fluorescence intensity of the polymer **P1** (lacking benzoic acid units) was not modified upon titration of CDs (up to 0.12 mM), which did not interact with the pyridyl receptors. Fig. 6(b)–(e) reveal that addition of CDs increased slightly the fluorescence intensities of the copolymers **P2** and **P3**, the blend (**P1/P4**) and the polymer **P4** in THF solutions. The optimal concentrations of CDs to capture the maximum number of hydrogen-bonded benzoic acid moieties in the polymer solutions—and, thereby, provide the highest PL intensities—were 0.02, 0.12, 0.05, and 0.12 mM for the copolymers **P2** and **P3**, the blend (**P1/P4**) and the homopolymer **P4**, respectively (PL emission enhancements: 1.09, 1.12, 1.08, and 1.16, respectively). Hence, the PL emission enhancements (1.16- and 1.12-fold) for the homopolymer **P4** and the copolymer **P3** were larger than those for the copolymer **P2** and the blend (**P1/P4**), due to the greater release of benzoic acid moieties after the addition of CDs to **P4** and **P3**, because the hydrogen-bonded benzoic acid moieties (bound as dimeric acids in the homopolymer **P4** or to pyridyl moieties in the copolymer **P3**) were capped with CDs to the largest extents.

Because the concentration of available (*i.e.*, non-hydrogen-bonded) pyridyl receptors for the sensing of metal ions could be adjusted by adding CDs, we investigated the fluorescence quenching effects of the polymers (with different molar ratios of **M1** and **M2** units) when titrated with Ni^{2+} ions in the presence of CDs. From the SV plots, the detection limits of polymers with CDs for Ni^{2+} ions were calculated to be in the range of 0.06–0.2 $\times 10^{-6}$ M. Fig. 7(a)–(d) display the fluorescence quenching spectra of the **P1** + CD, **P2** + CD, **P3** + CD, and blend (**P1/P4**) + CD systems, in THF, when titrated with the same concentration (up to 1.1×10^{-6} M) of Ni^{2+} ions. Compared with the fluorescence quenching spectra of the copolymers **P2** and **P3** in Fig. 4(a) and (b), the corresponding copolymer + CD systems (*i.e.*, **P2** + CD and **P3** + CD) were quenched more effectively upon titration with Ni^{2+} ions, because of the larger concentrations of available (*i.e.*, non-hydrogen-bonded) pyridyl receptors to sense the metal ions when CDs were present. Fig. 8(a)–(d) present SV plots—replotted from Fig. 7(a)–(d), respectively—of the **P1** + CD, **P2** + CD, **P3** + CD, and blend (**P1/P4**) + CD systems (in THF) titrated with the same concentration (up to 1.1×10^{-6} M) of Ni^{2+} ions; Table 3 lists their quenching constants (K_{SV}) extracted from the SV plots. After the addition of appropriate amounts of CDs to capture the benzoic acid moieties, the sensitivities of the fluorescent copolymers **P2** and **P3** towards Ni^{2+} ions improved, due to the increased concentration of non-hydrogen-bonded pyridyl receptors for metal ion sensing. Apart from the **P1** + CD system, which exhibited a decreased value of K_{SV} of 5.11×10^6 (because it possessed no benzoic acid moieties to interact with CDs), the addition of CDs caused the quenching constants of the **P2** + CD, **P3** + CD, and blend (**P1/P4**) + CD systems to increase to 4.76×10^6, 2.81×10^6, and 5.02×10^5 M^{-1}, respectively, due to the release of hydrogen-bonded pyridyl receptors. Compared with the blend (**P1/P4**) + CD system (*i.e.*, featuring a mixture of the homopolymers **P1** and **P4**), however, the copolymer **P2** + CD system [featuring a similar molar ratio of monomer units (x : y = 1 : 0.1)] had a larger Ni^{2+} ion sensitivity ($K_{SV} = 4.76 \times 10^6$), suggesting a greater concentration of available (*i.e.*, non-hydrogen-bonded) pyridyl receptors in the copolymer **P2** as a result of its weaker hydrogen bonding relative to that in the blend (**P1/P4**) + CD.

In order to verify this observation, FTIR and PL measurements of the copolymer **P2** and blend (**P1/P4**) are compared as shown in Fig. S2 and S3 of the ESI†. In contrast to the O–H bands of the pure donor homopolymer **P4** (H-bonded dimer) at 2660 and 2580 cm^{-1} in Fig. S2†, two new broad O–H bands centered at 2465 and 1920 cm^{-1} were observed in the H-bonded copolymer **P2** and blend (**P1/P4**), which revealed the existence of hydrogen bonding between the pyridyl and the carboxylic acid groups in the H-bonded networks of copolymer **P2** and blend (**P1/P4**). On the other hand, a stretching vibration of C=O at 1686 cm^{-1} in the pure homopolymer **P4** was shifted towards higher wavenumber and overlapped with the band of the ester carbonyl groups at 1725 cm^{-1} in the copolymer **P2** and blend (**P1/P4**), which showed that the carbonyl group was in a less associated state than that in the pure H-bonded dimer state of proton-donor **P4**. These FTIR results suggested that hydrogen-bonds were formed between **M1** and **M2** units in both the H-bonded copolymer **P2** and blend (**P1/P4**). Moreover, as illustrated in Fig. S3†, the stronger H-bonded effect of the blend

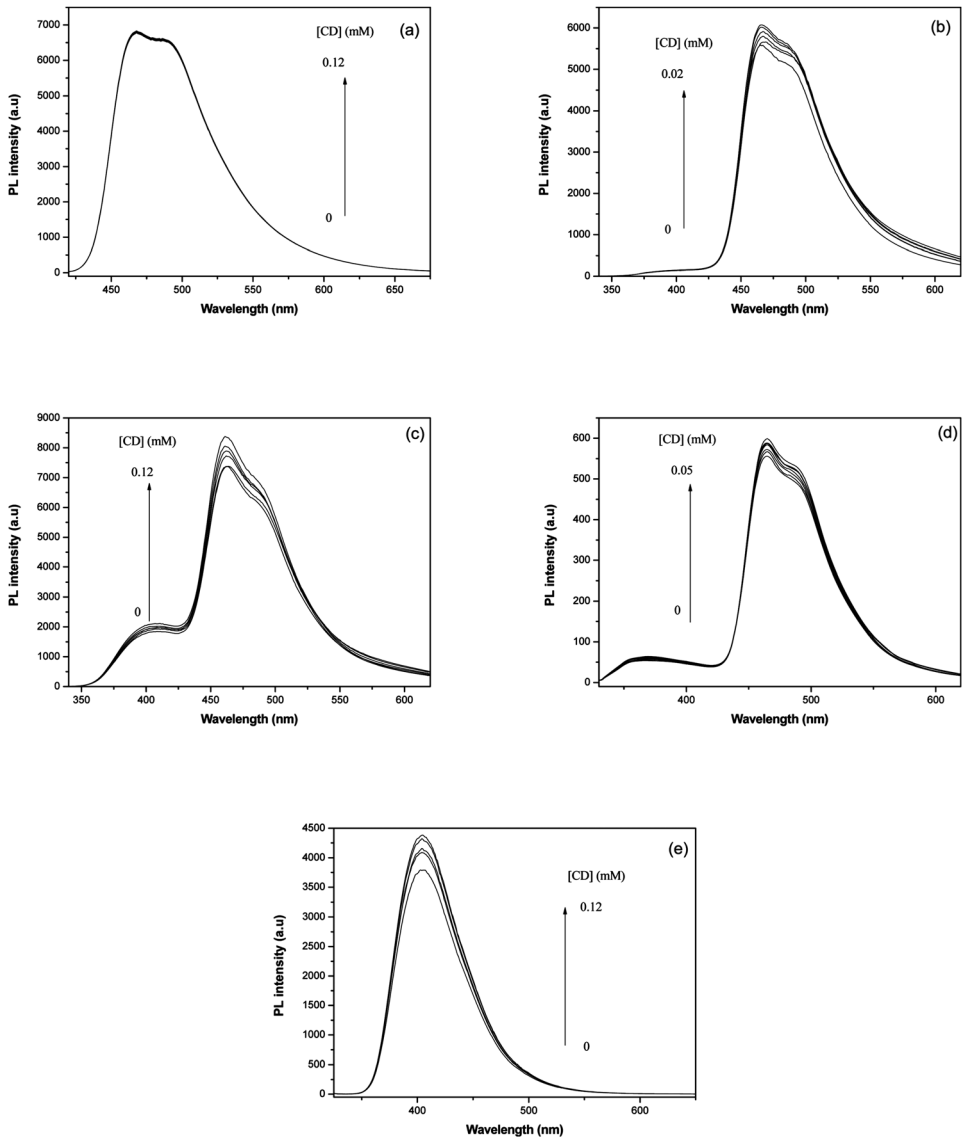

Fig. 6 Fluorescence quenching spectra of polymers in THF solutions (5×10^{-6} M), titrated with CDs (up to appropriate concentrations in parentheses): (a) **P1** (0.12 mM), (b) **P2** (0.02 mM), (c) **P3** (0.12 mM), (d) blend (**P1**/**P4**) (0.05 mM), and (e) **P4** (0.12 mM).

(**P1**/**P4**) could induce a more red-shifted PL emission in blend (**P1**/**P4**) than **P2**. Overall, the copolymer **P2** + CD system exhibited the largest Ni^{2+} ion sensitivity ($K_{SV} = 4.76 \times 10^6$) among all of our studied polymer + CD systems; it recovered almost all of its hydrogen-bonded pyridyl receptors after adding the CDs, reaching a Ni^{2+} ion sensitivity ($K_{SV} = 5.65 \times 10^6$) close to that of the homopolymer **P1**. Therefore, the sensitivity of Ni^{2+} ion detection becomes recoverable and/or adjustable through: (i) copolymer design, varying the molar ratio of hydrogen-bonding pyridyl receptors (proton-acceptor **M1** units) and benzoic acid moieties (proton-donor **M2** units) and (ii) the addition of CDs.

Time-resolved photoluminescence (TRPL) spectra

Heavy metal ions tend to quench the luminescence of conjugated receptors, including polymers and monomers, through electron-transfer and energy-transfer processes.[21–24] Comparing the fluorescence quenching spectra titrated with Ni^{2+} ions in Fig. 4 and 6, we observed that the ligation of the receptors in the polymers **P2**–**P4** and the **P2** + CD and **P3** + CD blends with metal ions (2.5×10^{-6} M) resulted in obvious quenching. Thus, we probed the time-resolved fluorescence (TRF) signals of the polymers **P2**–**P4** and the **P2** + CD and **P3** + CD systems at 480 nm upon excitation at 375 nm. Table 4 summarizes the fluorescence lifetimes obtained after deconvolution of the instrumental response function[25] and exponential fittings. The TRF traces of the polymers **P2**–**P4** in the absence/presence of metal ions, plotted in Fig. S4(a)–(c) of the ESI†, reveal that Ni^{2+} ions affected the fluorescence lifetimes of the copolymers **P2** and **P3** as a result of coordination with the pyridyl receptor moieties. In the absence of Ni^{2+} ions, a single exponential fitting provided fluorescence lifetimes (τ_2) for **P2**–**P4** of 1.296, 1.250, and 1.234 ns, respectively, corresponding to the lifetimes of their S1 states. Adding metal ions to the solutions caused another ultrafast decay time constant (τ_1) to appear in the results of bi-exponential decay fittings. The fluorescence lifetimes (τ_1) of **P2**–**P4** were 0.131, 0.173, and

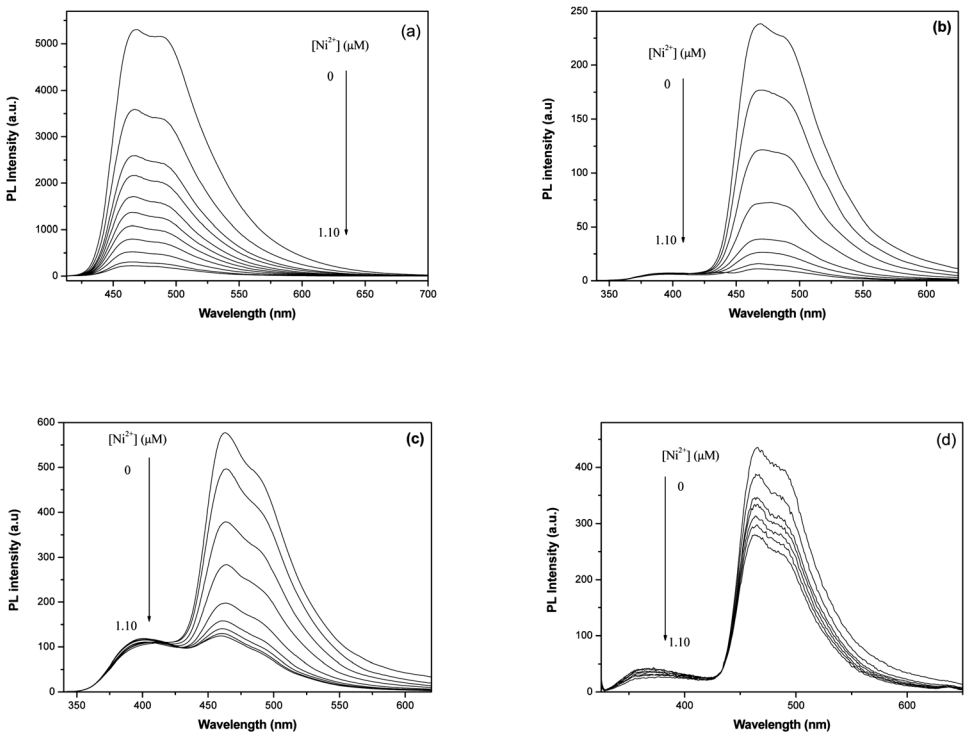

Fig. 7 Fluorescence quenching spectra of: (a) **P1** + CD, (b) **P2** + CD, (c) **P3** + CD, and (d) blend (**P1/P4**) + CD systems (in THF) titrated with the same concentration (up to 1.1×10^{-6} M) of Ni^{2+} ions.

0.208 ns, respectively. In the complex **P1** + Ni^{2+}, the ratio of the faster decay component increased up to 78.8% in the presence of Ni^{2+} ions,[18] reflecting the different interactions between the pyridyl receptor moieties of **P1** and Ni^{2+} ions. More importantly, the longer decay time constant (τ_2) of **P1** remained (27.8% for Ni^{2+} ions) even if Ni^{2+} ions were added to the solutions. The

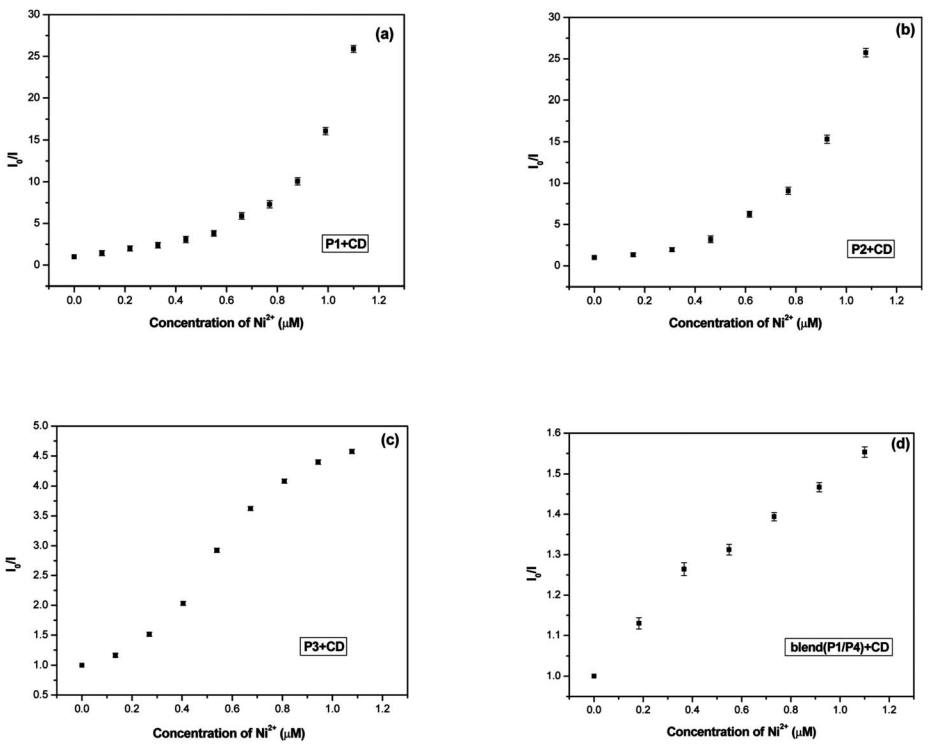

Fig. 8 SV plots of: (a) **P1** + CD, (b) **P2** + CD, (c) **P3** + CD, and (d) blend (**P1/P4**) + CD systems (in THF) titrated with the same concentration (up to 1.1×10^{-6} M) of Ni^{2+} ions.

Table 4 Fluorescence decay time constants for the polymers **P1–P4** and the **P2** + CD and **P3** + CD systems in the absence and presence of Ni^{2+} ions

Polymer	A_1	τ_1 (ns)	A_2	τ_2 (ns)
P1[a]			100%	1.375
P1 + Ni^{2+}[a]	78.8%	0.131	21.2%	1.578
P2			100%	1.296
P2 + Ni^{2+}	64.2%	0.173	35.8%	1.631
P3			100%	1.250
P3 + Ni^{2+}	40.1%	0.208	59.9%	1.542
P4			100%	1.234
P4 + Ni^{2+}			100%	1.234
P2 + CD			100%	1.516
P2 + CD + Ni^{2+}	70.2%	0.231	29.8%	1.622
P3 + CD			100%	1.325
P3 + CD + Ni^{2+}	55.2%	0.221	44.8%	1.576

[a] Lifetimes of **P1** and **P1** + Ni^{2+} were obtained from our previous report.[18]

emergence of the τ_1 decay component in the **P1** + Ni^{2+} system clearly indicates that its TRF traces featured two contributing factors: one (τ_2) from free **P1** and the other (τ_1) from its complex. The quenching of the TRF signals upon addition of Ni^{2+} implied that the metal ions formed a charge-transfer emitting state with **P1**. For the copolymers **P2** and **P3** in the presence of Ni^{2+} ions, we estimated their fluorescence lifetimes from bi-exponential fittings. Relative to that for the homopolymer **P1**, Table 4 reveals that the Ni^{2+} ions did not significantly affect the fluorescence decay times of the polymers **P2–P4**. We suggest that hydrogen bonding between the proton-acceptor pyridyl moieties (of monomer **M1** units) and proton-donor benzoic acid moieties (of monomer **M2** units) explains the similar fluorescence quenching effects on both the copolymers **P2** and **P3**. The decay time of the original decay component for the homopolymer **P4** could be approximately 100% of the longer decay time constant (τ_2) upon adding metal ions.[26] Moreover, as revealed in Fig. S4(d) and (e) of the ESI†, after adding appropriate amounts of CDs to the solutions of **P2** and **P3**, we used single-exponential fitting to estimate the fluorescence lifetimes of the **P1** + CD and **P2** + CD systems to be 1.516 and 1.325 ns, respectively; these values correspond to the lifetimes of the polymers. Relative to the copolymer **P2** + Ni^{2+} and **P3** + Ni^{2+} systems (without CDs), the faster components of the **P2** + CD + Ni^{2+} and **P3** + CD + Ni^{2+} systems (with CDs) increased from 64.2 and 40.1%, respectively, to 70.2 and 55.2%, respectively. The phenomena also proved that the quenching efficiencies of the copolymers **P2** and **P3** titrated with Ni^{2+} ions could be improved by adding CDs, and that these systems could be used as recoverable and/or adjustable chemosensors. Apparently, the interactions of the pyridyl receptors of the polymers with the Ni^{2+} ions created another fluorescence quenching pathway through which the photoexcitation energy of the pyridyl receptors was effectively transferred from the conjugated side chains to the Ni^{2+} ions. The observed fluorescence quenching phenomena of the ligands presumably reflect excitation energy transfer from the ligands to the metal ion's d orbital.[23,24] Therefore, with the addition of CDs, the disrupted hydrogen bonding between the pyridyl receptor moieties (of the proton-acceptor **M1** units) and the benzoic acid moieties (of the proton-donor **M2** units) in the copolymers enhanced the fluorescence quenching efficiencies of the Ni^{2+} ions in the fluorescence decay experiments, thereby facilitating the use of supramolecular side-chain copolymers as recoverable and/or adjustable chemosensors.

Conclusions

We have synthesized a series of fluorescent conjugated homopolymers (**P1** and **P4**) and copolymers (**P2** and **P3**) containing proton-acceptor (pyridyl) **M1** monomer units and proton-donor (benzoic acid) **M2** monomer units and studied their recoverable chemosensor sensitivities for metal ions (*via* adjustable fluorescence energy transfer between the **M1** and **M2** moieties with various degrees of hydrogen bonding). Among the tested metal ions, the homopolymer **P1** (containing only pyridyl receptors) exhibited its best chemosensing capability towards Ni^{2+} ions in fluorescence quenching experiments. Hence, we modified the concentrations of available (*i.e.*, non-hydrogen-bonded) pyridyl receptors through the design of copolymers **P2** and **P3** with different molar ratios of pyridyl **M1** and benzoic acid **M2** monomer units. We could distinguish the significant chelation interactions between the Ni^{2+} ions and the fluorescent homopolymers **P1** and **P4** and the copolymers **P2** and **P3** through their distinct fluorescence quenching behaviors; the specific quenching constants (K_{SV}) decreased in the order **P1** > **P2** > **P3** > **P4**, consistent with the trend of the decreasing molar ratios of their pyridyl receptors. Moreover, we introduced a third component, CDs, to cap the benzoic acid moieties and, thereby, disrupt the hydrogen bonding between the **M1** and **M2** moieties to different extents in the copolymers **P2** and **P3**. Accordingly, the concentrations of available pyridyl receptors in the recoverable chemosensor copolymers **P2** and **P3** were regained after capture of the benzoic acid moieties (of monomer **M2** units) by the CDs; as a result, the K_{SV} values of the **P2** + CD, **P3** + CD and blend (**P1**/**P4**) + CD systems all increased from 1.67×10^6, 4.91×10^5, and 3.72×10^5 M^{-1}, respectively, in the absence of CDs to 4.76×10^6, 2.81×10^6, and 5.02×10^5 M^{-1}, respectively, in the presence of CDs, due to the release of hydrogen-bonded pyridyl receptors. With the addition of CDs, the disrupted hydrogen bonding between the pyridyl receptor (**M1**) and benzoic acid (**M2**) moieties in the copolymers also enhanced the fluorescence quenching efficiencies of the Ni^{2+} ions in fluorescence decay experiments. Therefore, the developments of supramolecular (hydrogen-bonded) side-chain fluorescent copolymers (containing H-bonded moieties of **M1** and **M2**) might facilitate the future applications of recoverable (and/or adjustable) chemosensors by adding the third component of CDs.

Acknowledgements

We thank the National Science Council of Taiwan (NSC 99-2113-M-009-006-MY2) and National Chiao Tung University (97W807) for supporting this study financially.

Notes and references

1 (*a*) R. Martínez-Máñez and F. Sancenón, *Chem. Rev.*, 2003, **103**, 4419; (*b*) M. Royzen, A. Durandin, V. G. Young, N. E. Geacintov and J. W. Canary, *J. Am. Chem. Soc.*, 2006, **128**, 3854; (*c*) Z. C. Wen, R. Yang, H. He and Y. B. Jiang, *Chem. Commun.*,

2006, 106; (*d*) H. Yang, Z. Q. Liu, Z. G. Zhou, E. X. Shi, F. Y. Li, Y. K. Du, T. Yi and C. H. Huang, *Tetrahedron Lett.*, 2006, **47**, 2911; (*e*) G. Zhou, Y. Cheng, L. Wang, X. Jing and F. Wang, *Macromolecules*, 2005, **38**, 2148; (*f*) F. Du, H. Wang, Y. Bao, B. Liu, H. Zheng and R. Bai, *J. Mater. Chem.*, 2011, **21**, 10859.

2 (*a*) L. Basabe-Desmonts, D. N. Reinhoudt and M. Crego-Calama, *Chem. Soc. Rev.*, 2007, **36**, 993; (*b*) J. S. Kim and D. T. Quang, *Chem. Rev.*, 2007, **107**, 3780; (*c*) H. N. Lee, Z. Xu, S. K. Kim, K. M. K. Swamy, Y. Kim, S. J. Kim and J. Yoon, *J. Am. Chem. Soc.*, 2007, **129**, 3828; (*d*) P. Manoj, C. K. Min, C. T. Aravindakumar and T. Joo, *Chem. Phys.*, 2008, **352**, 333; (*e*) S. W. Thomas and T. M. Swager, *Macromolecules*, 2005, **38**, 2716; (*f*) A. K. Dwivedi, G. Saikia and P. K. Iyer, *J. Mater. Chem.*, 2011, **21**, 2502.

3 (*a*) C. B. Murphy, Y. Zhang, T. Troxler, V. Ferry, J. J. Martin and W. E. Jones, *J. Phys. Chem. B*, 2004, **108**, 1537; (*b*) L. J. Fan and W. E. Jones, *J. Am. Chem. Soc.*, 2006, **128**, 6784; (*c*) Z. Guo, W. Zhu, Y. Xiong and H. Tian, *Macromolecules*, 2009, **42**, 1448; (*d*) Q. Zou, L. Zou and H. Tian, *J. Mater. Chem.*, 2011, **21**, 14441; (*e*) H. Fan, T. Zhang, S. Lv and Q. Jin, *J. Mater. Chem.*, 2010, **20**, 10901.

4 (*a*) M. Royzen, Z. Dai and J. W. Canary, *J. Am. Chem. Soc.*, 2005, **127**, 1612; (*b*) M. Suresh, A. Ghosh and A. Das, *Chem. Commun.*, 2008, 3906; (*c*) K. M. K. Swamy, S. K. Ko, S. K. Kwon, H. N. Lee, C. Mao, J. M. Kim, K. H. Lee, J. Kim, I. Shin and J. Yoon, *Chem. Commun.*, 2008, 5915; (*d*) W. Hong, W. Li, X. Hu, B. Zhao, F. Zhang and D. Zhang, *J. Mater. Chem.*, 2011, **21**, 17193.

5 (*a*) N. Kaur and S. Kumar, *Chem. Commun.*, 2007, 3069; (*b*) H. N. Kim, M. H. Lee, H. J. Kim, J. S. Kim and J. Yoon, *Chem. Soc. Rev.*, 2008, **37**, 1465; (*c*) H. S. Jung, P. S. Kwon, J. W. Lee, J. I. Kim, C. S. Hong, J. W. Kim, S. Yan, J. Y. Lee, J. H. Lee, T. Joo and J. S. Kim, *J. Am. Chem. Soc.*, 2009, **131**, 2008; (*d*) T. Liu, J. Hu, J. Yin, Y. Zhang, C. Li and S. Liu, *Chem. Mater.*, 2009, **21**, 3439; (*e*) X. Wu, B. Xu, H. Tong and L. Wang, *Macromolecules*, 2011, **44**, 4241; (*f*) L. L. Li, H. Sun, C. J. Fang, J. Xu, J. Y. Jin and C. H. Yan, *J. Mater. Chem.*, 2007, **17**, 4492.

6 (*a*) J. P. Amara and T. M. Swager, *Macromolecules*, 2005, **38**, 9091; (*b*) J. Geng, B. S. Kong, S. B. Yang, S. C. Youn, S. Park, T. Joo and H. T. Jung, *Adv. Funct. Mater.*, 2008, **18**, 2659; (*c*) Z. A. Li, X. Lou, H. Yu, Z. Li and J. Qin, *Macromolecules*, 2008, **41**, 7433; (*d*) Y. Chen, F. Li and Z. Bo, *Macromolecules*, 2010, **43**, 1349; (*e*) D. J. Monk, J. Ueberfeld and D. R. Walt, *J. Mater. Chem.*, 2005, **15**, 4361.

7 (*a*) T. Gunnlaugsson, A. P. Davis, J. E. O'Brien and M. Glynn, *Org. Lett.*, 2002, **4**, 2449; (*b*) V. Thiagarajan, P. Ramamurthy, D. Thirumalai and V. T. Ramakrishnan, *Org. Lett.*, 2005, **7**, 657; (*c*) R. E. Gawley, H. Mao, M. M. Haque, J. B. Thorne and J. S. Pharr, *J. Org. Chem.*, 2007, **72**, 2187; (*d*) M. Kumar, A. Dhir and V. Bhalla, *Org. Lett.*, 2009, **11**, 2567.

8 (*a*) I. Grabchev, J. M. Chovelon and V. Bojinov, *Polym. Adv. Technol.*, 2004, **15**, 382; (*b*) B. Wang, Y. Hu and Z. Su, *React. Funct. Polym.*, 2008, **68**, 1137; (*c*) H. Y. Shi, B. Deng, S. L. Zhong, L. Wang and A. W. Xu, *J. Mater. Chem.*, 2011, **21**, 12309.

9 (*a*) Y. Cui, Q. Chen, D.-D. Zhang, J. Cao and B. H. Han, *J. Polym. Sci., Part A: Polym. Chem.*, 2010, **48**, 1310; (*b*) L. Shen, P. Zhao and W. Zhu, *Dyes Pigm.*, 2011, **89**, 236.

10 (*a*) E. Lippert, W. Lueder, F. Moll, W. Naegele, H. Boos, H. Prigge and I. Seibold-Blankenstein, *Angew. Chem.*, 1961, **73**, 695; (*b*) Z. R. Grabowski, K. Rotkiewicz, A. Siemiarczuk, D. J. Cowley and W. Baumann, *Nouv. J. Chim.*, 1979, **3**, 443; (*c*) W. Rettig, *Angew. Chem., Int. Ed. Engl.*, 1986, **25**, 971.

11 (*a*) G. S. Cox and N. J. Turro, *J. Am. Chem. Soc.*, 1984, **106**, 422; (*b*) K. Kasatani, M. Kawasaki and H. Safa, *J. Phys. Chem.*, 1984, **88**, 5451; (*c*) A. Nag and K. Bhattacharyya, *Chem. Phys. Lett.*, 1988, **151**, 474; (*d*) V. Ramamurthy and D. F. Eaton, *Acc. Chem. Res.*, 1988, **21**, 300; (*e*) S. Li and W. C. Purdy, *Chem. Rev.*, 1992, **92**, 1457; (*f*) K. A. Al-Hassan, U. K. A. Klein and A. Suwaiyan, *Chem. Phys. Lett.*, 1993, **212**, 581; (*g*) K. A. Al-Hassan, *Chem. Phys. Lett.*, 1994, **227**, 527; (*h*) N. Mataga, H. Yao, T. Okada and W. Rettig, *J. Phys. Chem.*, 1989, **93**, 3383.

12 (*a*) O. Kajimoto, M. Futakami, T. Kobyashi and K. Yamasaki, *J. Phys. Chem.*, 1988, **92**, 1347; (*b*) Y. P. Sun, M. A. Fox and K. P. Johnston, *J. Am. Chem. Soc.*, 1992, **114**, 1187; (*c*) Y. H. Kim, D. W. Cho, M. Yoon and D. Kim, *J. Phys. Chem.*, 1996, **100**, 15670.

13 P. R. Bangal, S. Panja and S. Chakravorti, *J. Photochem. Photobiol., A*, 2001, **139**, 5.

14 Y. B. Jiang and J. Photochem, *J. Photochem. Photobiol., A*, 1995, **88**, 109.

15 T. Stalin, B. Shanthi, V. Rani and N. Rajendiran, *J. Inclusion Phenom. Macrocyclic Chem.*, 2006, **55**, 21.

16 T. Stalin and N. Rajendiran, *J. Photochem. Photobiol., A*, 2006, **182**, 137.

17 T. Stalin and N. Rajendiran, *Chem. Phys.*, 2006, **322**, 311.

18 H. C. Chu, Y. H. Lee, S. J. Hsu, P. J. Yang, A. Yabushita and H. C. Lin, *J. Phys. Chem. B*, 2011, **115**, 8845.

19 K. W. Lee, K. H. Wei and H. C. Lin, *J. Polym. Sci., Part A: Polym. Chem.*, 2006, **44**, 4593.

20 P. J. Yang, C. W. Wu, D. Sahu and H. C. Lin, *Macromolecules*, 2008, **41**, 9692.

21 T. C. Liang and H. C. Lin, *J. Mater. Chem.*, 2009, **19**, 4753.

22 (*a*) K. W. Lee, K. H. Wei and H. C. Lin, *J. Polym. Sci., Part A: Polym. Chem.*, 2006, **44**, 4593; (*b*) P. J. Yang, C. W. Wu, D. Sahu and H. C. Lin, *Macromolecules*, 2008, **41**, 9692.

23 A. C. S. Samia, J. Cody, C. J. Fahrni and C. Burda, *J. Phys. Chem. B*, 2003, **108**, 563.

24 D. R. McMillin and K. M. McNett, *Chem. Rev.*, 1998, **98**, 1201.

25 S. Ishizaka, T. Wada and N. Kitamura, *Photochem. Photobiol. Sci.*, 2009, **8**, 562.

26 L. X. Chen, W. J. H. Jager, D. J. Gosztola, M. P. Niemczyk and M. R. Wasielewski, *J. Phys. Chem. B*, 2000, **104**, 1950.

